In summary, the nonrandom deletion of Xq in several immortal male Ni-transformed Chinese hamster cell lines suggested that this region of the X chromosome may harbor one or more senescence-inducing sequences, since microcell transfer of an intact Chinese hamster X chromosome resulted in dominant clonal senescence. Reintroduction of an active X chromosome may have complemented a genetic defect, possibly the loss of a growth regulatory gene. The high incidence of male transformations in Chinese hamsters suggested that inactivation of this senescence gene was important in Ni transformation and further suggested that female cells may be more resistant to transformation by this deletion mechanism if this gene was active in both of the female X chromosomes. Negative growth control has been attributed to a tumor suppressor gene (*18*), and repression of c-*fos* expression has been described in senescent human fibroblasts (*19*). The X chromosome has also been reported to be active in oncogenic transformation. A human synovial sarcoma with an X;18 translocation has been reported (*20*), and the *mcf-2* and A-*raf*-1 proto-oncogenes and tissue inhibitor of metalloproteinases, a putative suppressor gene, have been localized to the human X chromosome (*21*). The highly conserved nature of X chromosomal genes (*22*) suggests that the human X chromosome may also contain a senescence-inducing gene, and in preliminary experiments we have also observed senescing activity of the human X chromosome (*23*). Loss or inactivation of this senescence gene by hypermethylation may be associated with the acquisition of immortality, and may represent an early event associated with Ni-induced transformation.

REFERENCES AND NOTES

1. P. Armitage and R. Doll, *Br. J. Cancer* **8**, 1 (1954); A. G. Knudson, Jr., *Annu. Rev. Genet.* **20**, 231 (1986).
2. A. L. Murphree and W. F. Benedict, *Science* **223**, 1028 (1984); A. G. Knudson, Jr., *Cancer Res.* **45**, 1437 (1985).
3. R. Sager, *Science* **246**, 1406 (1989).
4. O. M. Periera-Smith and J. R. Smith, *Proc. Natl. Acad. Sci. U.S.A.* **85**, 6042 (1988).
5. O. Sugawara, M. Oshimura, M. Koi, L. A. Annab, J. C. Barrett, *Science* **247**, 707 (1990); H. Yamada *et al.*, *Oncogene* **5**, 141 (1990).
6. N. Nishioka, *Mutat. Res.* **31**, 185 (1975); N. Biggart and M. Costa, *ibid.* **175**, 209 (1986); P. Sen and M. Costa, *Cancer Res.* **45**, 2320 (1985); *Tox. Appl. Pharmacol.* **84**, 278 (1986).
7. K. Conway and M. Costa, *Cancer Res.* **49**, 6032 (1990).
8. M. Koi *et al.*, *Mol. Carcinogen.* **2**, 12 (1989); R. E. K. Fournier and F. H. Ruddle, *Proc. Natl. Acad. Sci. U.S.A.* **74**, 319 (1977); A. J. Saxon, E. S. Srivatsan, G. V. Leipzig, J. H. Sameshima, E. J. Stanbridge, *Mol. Cell. Biol.* **5**, 140 (1985).
9. R. G. Fenwick, Jr., *Somatic Cell Genet.* **6**, 477 (1980).
10. Microcell fusion: The X chromosome donor cells were seeded in 25-cm^2 flasks (Costar) 1 day before micronucleation. Micronuclei were induced by colcemid (0.05 μg/ml) in Dulbecco's modified Eagle's medium (DMEM) containing 20% fetal calf serum (FCS) for 48 hours. After the colcemid was removed, the flasks were replenished with warmed serum-free DMEM containing cytochalasin B (Sigma) (10 μg/ml) and centrifuged (12,000*g*, 30 min, 34°C) in an adaptor or a fixed-angle rotor with 100 ml of water in each rotor well. The microcell pellets were resuspended in serum-free DMEM and filtered through a series of 8-μm, 5-μm, and 3-μm polycarbonate filters (Nucleopore). The purified microcells were gently pelleted and resuspended in 3 ml of serum-free DMEM containing phytohemagglutinin (PHA) (50 or 100 μg/ml), then were overlaid onto the recipient cell monolayers and briefly incubated (15 min, 37°C). Microcell to cell fusion was accomplished in a solution of 47% polyethylene glycol (PEG) (w/w) (molecular weight 1600 to 1800; Sigma) for 1 min, followed by extensive washing in serum-free DMEM. After fusion, the recipient cells were incubated at 37°C in complete α-MEM media for 24 hours. The next day, recipient cells were trypsinized and replated at 1×10^6 cells per 100-mm dish with complete α-MEM containing HAT. The resulting HAT^R microcell hybrids were observed at 7 to 14 days after selection and were followed by microscopic and photographic evaluation of growth or senescence. Microcell hybrid colonies were recovered by this protocol at a frequency of 10^{-6}.
11. L. Hayflick and P. S. Moorehead, *Exp. Cell Res.* **25**, 585 (1961).
12. K. Conway, thesis, New York University Graduate School of Environmental Sciences (1989).
13. X. Wang, M. D. Cohen, M. Costa, unpublished observations.
14. J. M. Horowitz *et al.*, *Science* **243**, 937 (1989); R. Bookstein, J.-Y. Shew, P.-L. Chen, P. Scully, W.-H. Lee, *ibid.* **247**, 712 (1990); S. J. Baker *et al.*, *ibid.* **244**, 217 (1989); E. R. Fearon *et al.*, *ibid.* **247**, 49 (1990).
15. S. G. Grant and V. M. Chapman, *Annu. Rev. Genet.* **22**, 199 (1988).
16. C. J. Brown and H. F. Willard, *Am. J. Hum. Genet.* **46**, 273 (1990).
17. A. J. Hockey, C. N. Adra, M. W. McBurney, *Somatic Cell Mol. Genet.* **15**, 421 (1989).
18. M. Koi, C. A. Afshari, L. A. Annab, J. C. Barrett, *Proc. Natl. Acad. Sci. U.S.A.* **86**, 8733 (1989).
19. T. Seshadri and J. Campisi, *Science* **247**, 205 (1990).
20. K. Huebner, M. Isobe, J. C. Gasson, D. W. Golde, C. M. Croce, *Am. J. Hum. Genet.* **38**, 819 (1986); R. Khokha *et al.*, *Science* **243**, 947 (1989).
21. J. Limon, P. D. Cin, A. A. Sandberg, *Cancer Genet. Cytogenet.* **23**, 87 (1986); C. Turc-Carel *et al.*, *Proc. Natl. Acad. Sci. U.S.A.* **84**, 1981 (1987).
22. K. Huebner *et al.*, *Proc. Natl. Acad. Sci. U.S.A.* **83**, 3934 (1986); G. Stenman and R. Sager, *ibid.* **84**, 9099 (1987).
23. X. Wang and M. Costa, unpublished data.

24. We thank H. Satoh for karyotypic analysis of the A9-CX donor cells and some of the nonsenescing hybrids and M. Bader, A. Sandefur, and J. Galvin for preparation of the manuscript. This work was supported by grant R814702 from the U.S. Environmental Protection Agency and by grants ES 05512, ES 04715, and ES 04895 from the National Institute of Environmental Health Sciences.

26 July 1990; accepted 22 October 1990

Effect of Cytochrome P450 Arachidonate Metabolites on Ion Transport in Rabbit Kidney Loop of Henle

BRUNO ESCALANTE, DAVID ERLIJ, JOHN R. FALCK, JOHN C. MCGIFF

In the medullary segment of the thick ascending limb of the loop of Henle (mTALH), arachidonic acid (AA) is metabolized by a cytochrome P450–dependent monooxygenase to products that affect ion transport. The linkage between changes in ion transport and AA metabolism in isolated cells of the mTALH was examined. AA produced a concentration-dependent inhibition of ^{86}Rb uptake—an effect that was prevented by selective blockade of cytochrome P450 monooxygenases. Inhibition by cytochrome P450 blockade of the effect of AA on ^{86}Rb uptake could be circumvented by addition of the principal products of AA metabolism in the mTALH.

THE MEDULLARY SEGMENT OF THE thick ascending limb of the loop of Henle (mTALH) contributes to the regulation of extracellular fluid volume as indicated by its high capacity to reabsorb NaCl, thereby establishing the solute gradient for water reabsorption (*1*). The mTALH serves as the principal site of action of the most potent class of diuretic agents, which comprises furosemide and the other "loop" diuretic drugs (*1*). In cells isolated from the mTALH of the rabbit, arachidonic acid (AA) is specifically metabolized by a cytochrome P450–dependent pathway to one or more products that can affect Na^+- and K^+-dependent adenosine triphosphatase (Na^+,K^+-ATPase) activity when tested in vitro on cell membranes (*2, 3*). A local or circulating (*4, 5*) modulator of the Na^+,K^+-ATPase in vivo has long been sought. We propose that cytochrome P450 AA metabolites influence transport function locally in the mTALH.

In order to demonstrate that ion transport in intact mTALH cells is linked to AA metabolism, we studied the effects of cytochrome P450 AA metabolites on transport by measuring ^{86}Rb uptake in cells isolated from the mTALH and manipulating the flux of AA through the cytochrome P450 pathway. Movement of ^{86}Rb reflects that of K^+ and is a reliable estimate of ion

B. Escalante and J. C. McGiff, Department of Pharmacology, New York Medical College, Valhalla, NY 10595.
D. Erlij, Department of Physiology, State University of New York, Downstate Medical Center, Brooklyn, NY 11203.
J. R. Falck, Department of Molecular Genetics, University of Texas, Health Science Center, Dallas, TX 75235.

transport (*6*). The addition of AA to isolated mTALH cells inhibited ^{86}Rb uptake, and the effect was dependent on metabolism of AA by a cytochrome P450–related monooxygenase. Both inhibition of cytochrome P450 monooxygenase and depletion of cytochrome P450 blocked the effects of AA on ^{86}Rb uptake by mTALH cells. This blockade could be overcome by the addition of AA metabolites that we identified as products of cytochrome P450–dependent AA metabolism in mTALH cells (*7*).

A homogeneous population of isolated mTALH cells was prepared by an immunoaffinity procedure (*8*). Freshly adherent mTALH cells were fluorescently stained to visualize Tamm-Horsfall protein (Fig. 1). In six different experiments, 95 to 99% of cells were found to react with goat antibody to Tamm-Horsfall protein and fluorescein isothiocyanate–labeled rabbit antibody to goat immunoglobulin G (IgG). Freshly isolated mTALH cells, examined by transmission electron microscopy, had the appearance of mTALH cells in situ, with numerous mitochondria, large nuclei, and few or no microvilli (*8, 9*).

Incubation of mTALH cells with ^{14}C-labeled AA resulted in the formation of cytochrome P450 AA metabolites (Fig. 2, inset), which accounted for 10 to 15% of the recovered radioactivity. Formation of cytochrome P450 AA metabolites was not affected by the cyclooxygenase inhibitor indomethacin (7 μM). Separation by reverse-phase high-performance liquid chromatography (HPLC) revealed that the AA metabolites from immunoaffinity-purified mTALH cells had retention times indistinguishable from those of AA metabolites generated by mTALH cells isolated by centrifugal elutriation (*3*). Initially, we had reported that 5,6-epoxyeicosatetraenoic acid (5,6-EET) and 11,12-dihydroxyeicosatetraenoic acid, a product of 11,12-EET, could be identified in outer medullary cells isolated by centrifugal elutriation—a procedure yielding, on average, 80% mTALH cells (range of 65 to 90%) (*3*). The immunoaffinity procedure (*8*) virtually excludes cells from proximal tubules and collecting ducts, which have been reported to generate 5,6-EET and 11,12-EET, respectively (*10, 11*). Two products, 20-hydroxyeicosatetraenoic acid (20-HETE) and 20-carboxyarachidonic acid (20-COOH-AA) were identified with the aid of gas chromatography–mass spectrometry as principal products of AA metabolism in mTALH cells of the rabbit (*7*). The retention times on HPLC and the biological activities of authentic standards of 20-HETE and 20-COOH-AA were identical to those of the principal AA metabolites synthesized by immunoaffinity-purified mTALH cells (Fig. 2).

To assess activities of the Na^+,K^+-ATPase and the Na^+,K^+2Cl^- cotransporter in mTALH cells, we examined ^{86}Rb uptake in the presence and absence of 1 mM furosemide, which inhibits the cotransporter (*1*), and 1 mM ouabain, which inhibits the ATPase. ^{86}Rb uptake increased in a time-dependent manner and reached a saturation point in 5 to 10 min (Fig. 3). Both ouabain and furosemide inhibited ^{86}Rb uptake. Moreover, the inhibitory effects of furosemide and ouabain were not additive, which suggests that they act at different points in a common pathway.

Addition of AA (1 μM) significantly decreased the rate of ^{86}Rb uptake (Fig. 4) in a concentration-dependent manner. The effect of AA on ^{86}Rb uptake was blocked by eicosatetraynoic acid (ETYA) (30 μM) (Fig. 4, inset), which is a competitive inhibitor of AA metabolism by all pathways (*12*); thus presumably AA has to be metabolized by mTALH cells in order for it to inhibit ^{86}Rb uptake. Indomethacin (1 μM) did not affect the action of AA on ^{86}Rb uptake (Fig. 4, inset). However, inhibition of the cytochrome P450 pathway with SKF 525A (100 μM) blocked the effect of AA on ^{86}Rb uptake (Fig. 4, inset), suggesting that AA metabolites generated by the cytochrome P450 pathway mediate the AA effect (*2*). Indomethacin and SKF 525A had no effect on ^{86}Rb uptake in the absence of added AA.

To confirm the role of the cytochrome

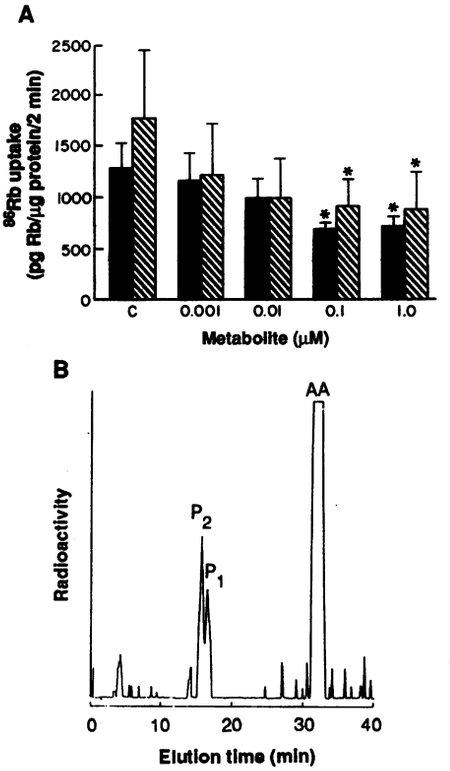

Fig. 2. (**A**) Concentration-dependent effect of authentic AA metabolites of the cytochrome P450 pathway on ^{86}Rb uptake. Isolated mTALH cells were incubated with various concentrations of either 20-HETE (striped bar) (n = 4) or 20-COOH-AA (solid bar) (n = 4) for 10 min. ^{86}Rb (1 μCi) was added 2 min before measurement of uptake. Each bar represents the mean ± SEM. Significance of inhibition of ^{86}Rb uptake (expressed as a percentage) by 20-HETE and 20-COOH-AA, compared with control (C), was determined by analysis of variance and Newman Keuls' test (*, $P < 0.05$). (**B**) HPLC chromatogram of AA metabolites formed by mTALH cells. The retention times of peaks 1 and 2 (P_1 and P_2) correspond to those of authentic standards of 20-HETE and 20-COOH-AA (*7*).

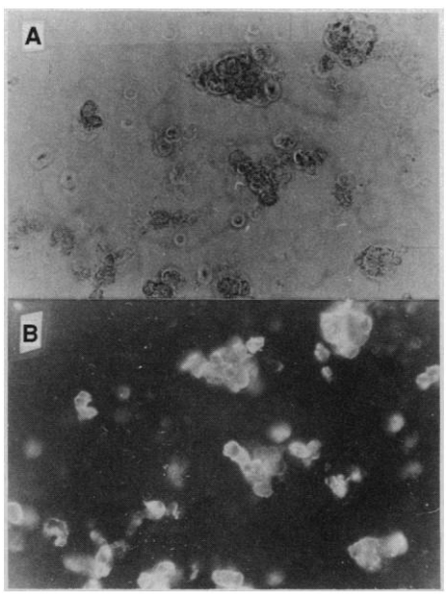

Fig. 1. Detection of Tamm-Horsfall protein in isolated mTALH cells. (**A**) Phase-contrast photomicrograph of immunoaffinity-prepared mTALH cells adsorbed to the surface of a culture dish coated with antibodies to goat immunoglobulin G (IgG). (**B**) Fluorescence photomicrograph of the field shown in (A) (see text). Cells were prepared essentially as described (*8*). New Zealand White rabbits (1 to 1.5 kg) were anesthetized with sodium pentobarbital (30 mg per kilogram of body mass). The inner stripe of the kidney outer medulla was cut into strips, finely diced in Hanks' buffer Krebs (HBK) containing 0.1% collagenase, and incubated at 37°C for 30 min in 20 ml of 0.1% collagenase–HBK (pH 7.4). After dispersion, the sample was centrifuged at 300g for 5 min and the supernatant removed. The cell pellet was suspended in 10 ml of Dulbecco's modified Eagle's medium (DMEM) containing 10 mM Hepes (pH 7.4) and 125 μl of goat antiserum to human uromucoid (50 mg of protein per milliliter) (Organon Teknika; lot 33185), and incubated for 20 min on ice. After a further centrifugation, the cells were resuspended in 5 ml of phosphate-buffered saline (PBS); 1 ml of the suspension was added to each of five 100-mm-diameter culture dishes coated with donkey antibodies to goat IgG (Sigma; lot 18F8812) for 5 min at 24°C. The dishes were then washed with PBS and the suspended tubules and cells were collected by centrifugation.

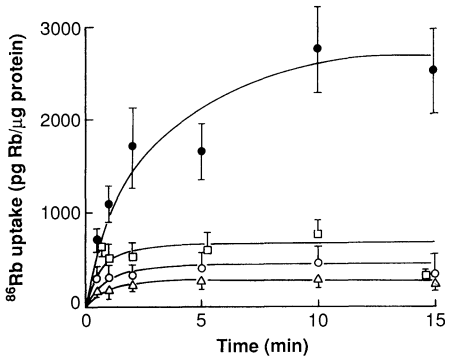

Fig. 3. Effect of furosemide and ouabain on ^{86}Rb uptake by mTALH cells. Cells were incubated with 1 mM furosemide (n = 3) (□), 1 mM ouabain (n = 3) (△), furosemide and ouabain (n = 3) (○), or solvent (n = 7) (●) for 10 min before addition of ^{86}Rb at time zero. Uptake was stopped after various times and radioactivity measured. Each value represents the mean ± SEM. Freshly isolated cells (40 to 80 μg of protein per milliliter) were incubated on ice for 20 min in K^+-free Hanks' balanced salt solution (*6, 16*): 136.8 mM NaCl, 1.26 mM $CaCl_2$, 0.49 mM $MgCl_2$, 0.33 mM NaH_2PO_4, 4.16 mM $NaHCO_3$, and 5.5 mM glucose. Uptake was initiated by adding ^{86}Rb (1 μCi) (specific activity, 0.3 μg/μCi) and K^+ (to give a final concentration of 5 mM) to 1 ml of cell suspension in a shaking water bath at 37°C. At the indicated time points, 200-μl portions of the cell suspensions were added to 75 μl of Hanks' balanced salt solution, 75 μl of silicone oil, and 75 μl of dioctylphthalamate. The cells were centrifuged through the oil (13,000*g* for 30 s), the supernatant was discarded, and the radioactivity present in the cell pellet was determined in a scintillation counter. The pellets were homogenized and their protein content was measured.

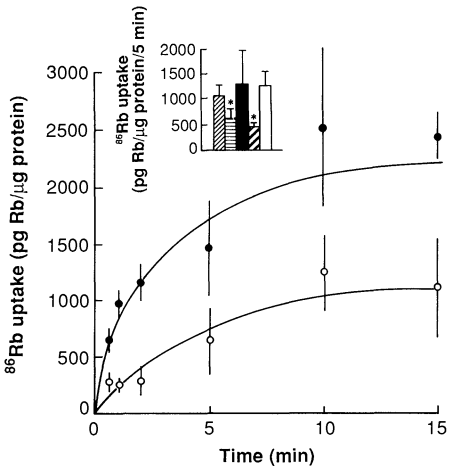

Fig. 4. Effect of AA on ^{86}Rb uptake. Cells were incubated with 1 μM AA (n = 5) (○) or solvent alone (●) for 10 min. ^{86}Rb was added at time zero; uptake was stopped after various times and radioactivity measured. Each point represents the mean ± SEM. (Inset) Effect of inhibitors of AA metabolism on ^{86}Rb uptake. Cells were incubated with solvent (n = 21) (thin diagonal stripes), 1 μM AA (n = 23) (horizontal stripes), 30 μM ETYA plus 1 μM AA (n = 6) (solid bar), 1 μM indomethacin plus 1 μM AA (n = 5) (thick diagonal stripes), and 100 μM SKF 525A plus 1 μM AA (n = 5) (open bar). ^{86}Rb uptake was measured 5 min after addition of ^{86}Rb (1 μCi). Each bar represents the mean ± SEM. Significance compared with solvent control was determined by analysis of variance and Newman Keuls' test (*, $P < 0.05$).

P450 system in mediating the effect of AA on ^{86}Rb uptake, we depleted mTALH cells of cytochrome P450—which reduces the metabolism of AA by mTALH cells (*13*). This was achieved with $CoCl_2$, which induces heme oxygenase activity and thereby enhances the catabolism of cytochrome P450 and other heme-containing enzymes (*14*). Rabbits were treated with $CoCl_2$ (50 mg per kilogram of body mass) (*13*) or saline solution for 2 days. In mTALH cells prepared from saline-treated rabbits, AA produced a concentration-dependent inhibitory effect on ^{86}Rb uptake, whereas in mTALH cells prepared from $CoCl_2$-treated rabbits, AA had no effect on ^{86}Rb uptake (n = 3). The effect of $CoCl_2$ on the action of AA was related to a >60% decrease in the ability of mTALH cells to metabolize AA by the cytochrome P450 pathway [1.239 ± 0.483 and 0.524 ± 0.267 μg of AA converted per milligram of protein per 5 min for cells from saline-treated and $CoCl_2$-treated rabbits, respectively (mean ± SEM values, n = 3)].

Both 20-HETE and 20-COOH-AA inhibited ^{86}Rb uptake in a concentration-dependent manner (Fig. 2). Further, when we tested these metabolites on mTALH cells from $CoCl_2$-treated rabbits, in which AA (1 μM) was without effect on ^{86}Rb uptake, both metabolites inhibited ^{86}Rb uptake [391 ± 67, 372 ± 54, 172 ± 69, and 157 ± 64 pg of ^{86}Rb per microgram of protein per 2 min (mean ± SEM, n = 3) for control, AA (1 μM), 20-HETE (1 μM), and 20-COOH-AA (1 μM), respectively].

Thus, our experiments show that immunoaffinity-purified mTALH cells provide a suitable system in which to evaluate the activity of the Na^+,K^+-ATPase. Inhibition by ouabain indicates that more than 80% of the ^{86}Rb uptake in these cells is mediated through the Na^+,K^+-ATPase. Inhibition of ^{86}Rb uptake by furosemide presumably is related to a secondary effect of the drug on the Na^+,K^+-ATPase. Furosemide is known to block the Na^+,K^+2Cl^- cotransporter that mediates Na^+ entry into mTALH cells (*1*). Because Na^+,K^+-ATPase activity is driven by the cytoplasmic Na^+ concentration, any procedure that interferes with Na^+ entry into the cell will reduce the activity of the pump. Similar inhibitory effects of ouabain and furosemide on O_2 consumption by mTALH cells have been described (*9*). Because the rate of O_2 consumption is driven by adenosine triphosphate (ATP) hydrolysis and because a major fraction of ATP hydrolysis in mTALH cells reflects the activity of the Na^+,K^+-ATPase, the observed inhibition of O_2 consumption by ouabain and furosemide is in agreement with our conclusion that these agents affect Na^+,K^+-ATPase activity (*15, 16*). We have also found that ouabain and furosemide, as well as AA, inhibit O_2 consumption in mTALH (*17*).

Thus, our results show that AA inhibits ^{86}Rb uptake in mTALH cells, an effect which is mediated by AA metabolites that are generated through a cytochrome P450–dependent pathway. Because the results obtained with furosemide indicated that blocking the Na^+,K^+2Cl^- cotransporter can also lead to an inhibition of ^{86}Rb uptake, our findings are insufficient to identify whether the primary effect of AA metabolites is on the Na^+,K^+-ATPase, the cotransporter, or, possibly, both. In order to define the principal site of action of mTALH AA metabolites, we compared the effects of 20-HETE and 20-COOH-AA to those of furosemide and ouabain on Na^+ and K^+ content of mTALH cells. The effects of cytochrome P450 AA metabolites resembled that of furosemide: they decreased both the Na^+ and K^+ concentration of mTALH cells. In contrast, ouabain increased the Na^+ concentration and decreased that of K^+ (*18*). The products of AA metabolism by cytochrome P450, therefore, appear to affect the transport function of mTALH cells by virtue of affecting the Na^+,K^+2Cl^- cotransporter. An inhibitory effect on the cotransporter should result in natriuresis and diuresis, a result that has been recently reported for 20-HETE (*19*).

REFERENCES AND NOTES

1. R. Kinne, in *Renal Biochemistry*, R. K. H. Kinne, Ed. (Elsevier, Amsterdam, 1985), pp. 99–141.
2. N. R. Ferreri, M. Schwartzman, N. G. Ibraham, P. N. Chander, J. C. McGiff, *J. Pharm. Exp. Therap.* **231**, 441 (1984).
3. M. Schwartzman, N. R. Ferreri, M. A. Carroll, E. Songu-Mize, J. C. McGiff, *Nature* **314**, 620 (1985).
4. A. I. Katz, *Am. J. Physiol.* **242**, F207 (1982).
5. H. W. Overbeck, M. B. Pamnani, T. Akera, T. M. Brody, F. J. Haddy, *Circ. Res.* **38**, 48 (1976).
6. I. Seri *et al.*, *Am. J. Physiol.* **255**, F666 (1988).
7. We obtained large quantities of AA products (extracted but not purified) from mTALH cells that were pooled from 20 rabbits; [^{14}C]AA (1 μM) and unlabeled AA (6 μM) were incubated with each of the 20 samples before pooling. Reverse-phase high-performance liquid chromatography (HPLC) separated labeled AA metabolites into two major and five minor peaks; ω-oxidation products predominated in the major peaks. Structural analysis of the major peaks based on gas chromatography–mass spectrometry revealed the presence of 20-hydroxyeicosatetraenoic acid (20-HETE) in the less polar peak and the presence of 20-carboxyarachidonic acid (20-COOH-AA) in the more polar peak.

8. M. L. Allen *et al.*, *Am. J. Physiol.* **255**, F704 (1988).
9. M. E. Chamberlin *et al.*, *ibid.* **247**, F955 (1984).
10. M. F. Romero, Z. T. Madhun, U. Hopfer, J. G. Douglas, in *Advances in Prostaglandins, Thromboxane, and Leukotriene Research. Prostaglandins and Related Compounds*, B. Samuelsson, R. Paoletti, P. W. Ramwell, Eds. (Raven, New York, 1990), pp. 205–208.
11. D. L. Hirt, J. Capdevila, J. R. Falck, M. D. Breyer, H. R. Jacobson, *J. Clin. Invest.* **84**, 1805 (1989).
12. D. T. Downing, D. G. Ahern, M. Bachta, *Biochem. Biophys. Res. Commun.* **40**, 218 (1970).
13. M. L. Schwartzman, N. G. Abraham, M. A. Carroll, R. D. Levere, J. C. McGiff, *Biochem. J.* **238**, 283 (1986).
14. M. D. Maines, N. G. Ibrahim, A. Kappas, *J. Biol. Chem.* **252**, 5900 (1977).
15. J. Eveloff, E. Bayerdorffer, P. Silva, R. Kinne, *Pflügers Arch.* **389**, 263 (1981).
16. H. F. Cantiello, E. Chen, S. Ray, G. T. Haupert, *Am. J. Physiol.* **255**, F574 (1988).
17. O_2 consumption was measured in mTALH cells with the use of a Clark-type electrode (*9*). O_2 consumption was inhibited by ouabain from 220 ± 4 to 153 ± 3 nmol O_2 per 5×10^6 cells per minute and by furosemide from 289 ± 20 to 181 ± 23 nmol O_2 per 5×10^6 cells per minute (mean ± SEM values; $n = 6$), indicating that in mTALH cells a large part of O_2 consumption is driven by ion transport. AA (1 μM) reduced O_2 consumption from 324 ± 22 to 201 ± 19 nmol O_2 per 5×10^6 cells per minute (mean ± SEM values; $n = 7$). Synthetic 20-HETE and 20-COOH-AA standards also decreased O_2 consumption from 254 ± 10 to 160 ± 12 (mean ± SEM values; $n = 11$) and from 260 ± 8 to 190 ± 9 nmol O_2 per 5×10^6 cells per minute (mean ± SEM values; $n = 7$), respectively.
18. Ion content of mTALH cells was measured by flame photometry after treatment with ouabain and furosemide for 15 min or with 20-HETE and 20-COOH-AA for 5 min. Ouabain (1 mM) increased Na^+ by 50 ± 8% and decreased K^+ by 50 ± 7%; whereas furosemide (1 mM) decreased Na^+ and K^+ by 49 ± 7% and 46 ± 5%, respectively (mean ± SEM values; $n = 6$). 20-HETE (1 μM) decreased both Na^+ and K^+ by 58 ± 14% and 24 ± 3%, respectively; 20-COOH-AA (1 μM) decreased both Na^+ and K^+ by 35 ± 6% and 25 ± 17%, respectively (mean ± SEM values; $n = 4$). Changes in the concentration of Na^+ and K^+ were significantly different ($P < 0.05$) from control values by analysis of variance and Newman Keuls' test.
19. K. Takahashi *et al.*, *Am. J. Physiol.* **258**, F781 (1990).
20. The AA metabolites generated in mTALH cells were purified and identified structurally in the laboratory of R. C. Murphy. We thank J. Jones for typing the manuscript and M. Steinberg for editorial assistance.
Supported by NIH Program Project Grant HL34300, and NIH grants R01 HL25394 (J.C.M.), R01 DK33612 (D.E.), and JM31278 (J.R.F.).

30 May 1990; accepted 26 November 1990

Identification of the Hepatocyte Growth Factor Receptor as the c-*met* Proto-Oncogene Product

DONALD P. BOTTARO, JEFFREY S. RUBIN, DONNA L. FALETTO, ANDREW M.-L. CHAN, THOMAS E. KMIECIK, GEORGE F. VANDE WOUDE, STUART A. AARONSON

Hepatocyte growth factor (HGF) is a plasminogen-like protein thought to be a humoral mediator of liver regeneration. A 145-kilodalton tyrosyl phosphoprotein observed in rapid response to HGF treatment of intact target cells was identified by immunoblot analysis as the β subunit of the c-*met* proto-oncogene product, a membrane-spanning tyrosine kinase. Covalent cross-linking of ^{125}I-labeled ligand to cellular proteins of appropriate size that were recognized by antibodies to c-*met* directly established the c-*met* product as the cell-surface receptor for HGF.

HEPATOCYTE GROWTH FACTOR (HGF) was first purified from human and rabbit plasma and rat platelets on the basis of its ability to stimulate mitogenesis of rat hepatocytes (*1–3*). Thus, HGF may act as a humoral factor promoting liver regeneration after partial hepatectomy or liver injury (*4*). The same factor was purified from human fibroblast culture medium and shown to act on melanocytes and a variety of epithelial and endothelial cells (*5*). Together with evidence of HGF expression in several organs (*5–8*), these findings indicate that HGF may also act as a paracrine mediator of proliferation for a broad spectrum of cell types. Molecular cloning of HGF revealed structural similarity to plasminogen and related serine proteases (*5, 9, 10*). Recent evidence that HGF induces rapid tyrosine phosphorylation of proteins in intact target cells suggests that a tyrosine kinase receptor might mediate its mitogenic signal (*5*).

The human mammary epithelial cell line B5/589 is particularly sensitive to the mitogenic effects of HGF (*5*). Intact serum-starved B5/589 cells were treated with HGF (approximately 100 ng/ml) for 10 min at 37°C and solubilized on ice. Phosphotyrosyl proteins were isolated from cell lysates by immunoprecipitation with antibody to phosphotyrosine (anti-pTyr). These proteins were resolved by SDS–polyacrylamide gel electrophoresis (SDS-PAGE) and immunoblotted with the same antibody. Several phosphotyrosyl proteins were detected in untreated cells by this method (Fig. 1A). Treatment of intact cells with HGF induced phosphorylation of a 145-kD protein (p145) (Fig. 1A, center lane). B5/589 cells exposed to epidermal growth factor (EGF) displayed tyrosine phosphorylation of the EGF receptor, but not p145 (Fig 1A, right lane). When lysates from control and HGF-treated cells that had been labeled with [^{32}P]orthophosphate were used for immunoprecipitation with anti-pTyr, phosphorylation of p145 was specifically detected in HGF-treated cells (Fig. 1B). Phosphoamino acid analysis of ^{32}P-labeled p145 confirmed the presence of phosphotyrosine and revealed the presence of phosphoserine as well (Fig. 1C). The HGF-stimulated phosphorylation of p145 on tyrosine and its apparent molecular weight were consistent with the possibility that p145 represented the receptor tyro-

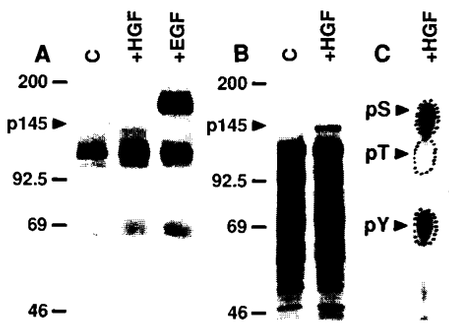

Fig. 1. Tyrosine phosphorylation of p145 in B5/589 human mammary epithelial cells in response to HGF. (**A**) Immunoblot of phosphotyrosyl proteins from untreated control cells (C), treated with HGF, and with EGF (Collaborative Research). HGF was purified as described (*5*). Serum-starved cells were exposed to growth factor (100 ng/ml) for 10 min at 37°C as indicated, detergent-solubilized on ice, and immunoprecipitated with monoclonal antibody to pTyr (Upstate Biotechnology). Immunoprecipitated proteins were resolved by 7.5% SDS-PAGE (*30*) and immunoblotted with the same antibody (*31*). (**B**) Autoradiogram of ^{32}P-labeled phosphoproteins from control (C) and HGF-treated cells. Serum-starved cells were metabolically labeled with [^{32}P]orthophosphate (1.0 mCi/ml) (*32*). The cells were treated with HGF (100 ng/ml) for 10 min at 37°C as indicated and detergent-solubilized on ice. Phosphotyrosyl proteins were immunoprecipitated with anti-pTyr and resolved by 7.5% SDS-PAGE. (**C**) Phosphoamino acid analysis of p145 from lane 2 of (B) was performed as described (*32*). The dotted circles indicate the migration of unlabeled phosphoserine (pS), phosphothreonine (pT), and phosphotyrosine (pY).

D. P. Bottaro, J. S. Rubin, A. M.-L. Chan, S. A. Aaronson, Laboratory of Cellular and Molecular Biology, National Cancer Institute, Bethesda, MD 20892.
D. L. Faletto, T. E. Kmiecik, G. F. Vande Woude, ABL–Basic Research Program, NCI–Frederick Cancer Research and Development Center, Frederick, MD 21702.